Design and Synthesis of α-Aryloxyphenylacetic Acid Derivatives: A Novel Class of PPARα/γ Dual Agonists with Potent Antihyperglycemic and Lipid Modulating Activity

Guo Q. Shi,*,† James F. Dropinski,† Brian M. McKeever,† Shihua Xu,† Joseph W. Becker,† Joel P. Berger,‡ Karen L. MacNaul,‡ Alex Elbrecht,‡ Gaochao Zhou,‡ Thomas W. Doebber,‡ Peiran Wang,§ Yu-Sheng Chao,§ Mike Forrest,# James V. Heck,† David E. Moller,‡ and A. Brian Jones†

Departments of Medicinal Chemistry, Metabolic Disorders, Atherosclerosis and Endocrinology and Animal Pharmacology, Merck Research Laboratories, P.O Box 2000, Rahway, New Jersey 07065-0900

Received March 8, 2005

The synthesis and structure−activity relationships of novel series of α-aryloxyphenylacetic acids as PPARα/γ dual agonists are reported. The initial search for surrogates of the ester group in the screen lead led first to the optimization of a subseries with a ketone moiety. Further efforts to modify the ketone subseries led to the design and synthesis of two new subseries containing fused heterocyclic ring systems. All these analogues were characterized by their "super" PPARα agonist activity and weak or partial agonist activity on PPARγ in PPAR-GAL4 transactivation assays despite their similar binding affinities for both receptors. The cocrystal structures of compounds **7** and rosiglitazone with PPARγ-LBD were compared, and significant differences were found in their interactions with the receptor. Select analogues in each subseries were further evaluated for in vivo efficacy. They all showed excellent anti-hyperglycemic efficacy in a *db*/*db* mouse model and hypolipidemic activity in hamster and dog models without provoking the typical PPARγ-associated side effects in the rat tolerability assay.

Introduction

The peroxisome proliferator-activated receptors (PPARs) are ligand-activated transcription factors in the nuclear hormone receptor superfamily.[1,2] Three distinct PPAR subtypes (PPARγ, PPAα and PPARδ) have been identified in most mammalian species. The physiological role of the PPARs as regulators of lipid and glucose metabolism has been extensively reviewed in recent years.[3−7] PPARγ is well-known at a cellular level for its role in adipogenesis and has been implicated as the primary receptor modulating the antidiabetic activity through insulin sensitization.[8,9] PPARγ agonists, such as TZDs, have proven to be efficacious as insulin sensitizing agents in the treatment of type 2 diabetes.[10−12] Unfortunately, they are also known to cause undesirable side effects including weight gain (as a result of enhanced adipogenisis and increased plasma volume), edema and anemia in both animal models and humans. PPARα is known to play a pivotal role in the uptake and oxidation of fatty acids and also in lipoprotein metabolism.[13] Activation of PPARα is known to be the predominant mechanism by which fibrates lower triglycerides, elevate HDL and exert insulin sensitizing effects.[14−20] Since the majority of type 2 diabetes patients suffer from atherogenic lipid abnormalities in addition to insulin resistance, both of which are maladies associated with the so-called metabolic syndrome,[21] the concept of identifying ligands that activate both PPARα and PPARγ represents a logical continuation in the field of PPAR research.

Chart 1. Chemical Structures of Selected PPARα/γ Dual Agonists

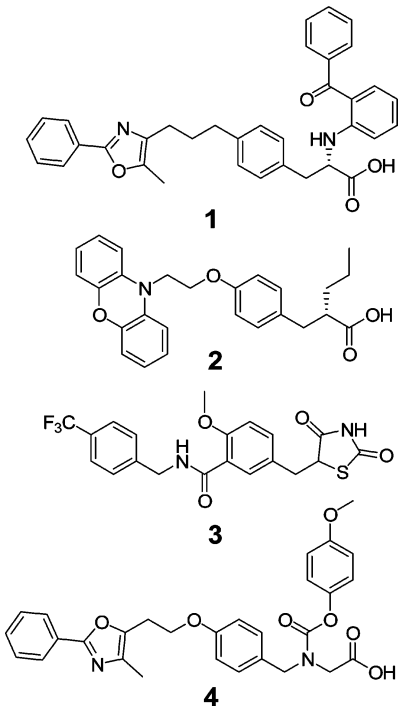

Indeed, there have been intense efforts within the pharmaceutical industry to develop PPARα/γ dual agonists for clinical use (Chart 1).[22−33] The first example, compound **1** (farglitazar),[23] a potent PPARγ agonist with a moderate PPARα component, was developed as a clinical candidate but was dropped due to the emergence

* To whom correspondence should be addressed. Tel: 732-594-8592; Fax: 732-5949556; e-mail: guoqiang_shi@merck.com.
† Department of Medicinal Chemistry.
‡ Metabolic Disorders.
§ Atherosclerosis and Endocrinology.
# Animal Pharmacology.

10.1021/jm0502135 CCC: $30.25
Published on Web 06/04/2005

Chart 2

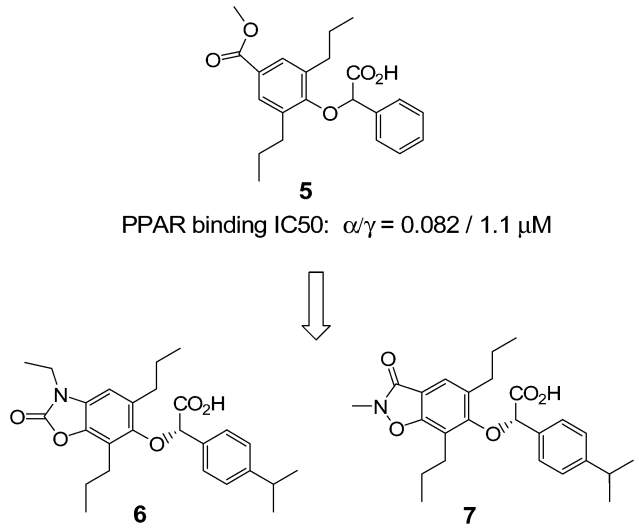

of edema in an advanced stage of development. Two dual agonists with more substantial PPARα activity, **2** (ragaglitazar or DRF2725)[25] and **3** (MK-767 or KRP-297),[24] were also dropped from late clinical development due to carcinogenicity in rodent toxicity models. So far, compound **4** (muraglitazar)[28,33] is the only dual agonist candidate that has been successfully advanced to NDA filing.[34] Thus, the development of PPARα/γ dual agonists with novel biological profiles and structural diversity remains an attractive field for further exploration.

Our research on PPARα/γ dual agonists was initiated from the screening lead **5**, which possessed a unique molecular architecture (Chart 2). It was a phenylacetic acid substituted at the α-position with a phenoxy group, to which was symmetrically attached two propyl groups on each side and an ester group at the para position. This structural feature differentiates compound **5** from most existing PPARα/γ dual agonists reported in the literature, which are frequently represented by an amphiphilic molecular design including an acidic "head-group" tethered with a chain to a lipophilic "tail group", such as those shown in Chart 1. Compound **5** was discovered as a PPAR ligand with micromolar hPPARγ and nanomolar hPPARα affinity (PPAR_SPA IC_{50}: α/γ = 0.082/1.1 μM). In the cell-based PPAR-GAL4 chimera transactivation assay (TA) assay, this compound turned out to be a "super" agonist [35] for hPPARα and a weak agonist for hPPARγ receptors. The novel structural features of compound **5** coupled with its interesting in vitro biological profile prompted us to embark on further investigation. A preliminary report describing some early structure−activity studies has appeared.[31] This paper describes the synthesis, the SAR development, X-ray crystallography study and various in vivo evaluations of a new series of α-aryloxyphenylacetic acids that culminated in the discovery of compound **6** and **7**.

Chemistry

Most compounds in the racemic series were readily synthesized by S_N2 coupling between α-bromophenylacetates and three different types of phenols (Scheme 1). For the synthesis of the enantiomerically pure analogues, a highly stereoselective synthetic route based on the use of a lactate-derived chiral auxiliary **9** was adopted.[36] Thus, the readily available phenylglyoxalic acid **8** was esterified with chiral auxiliary **9**, and the resulting keto ester **10** was converted to the α-bromo ester **11** as a diastereomeric mixture. Displacement of the bromide by various lithium phenoxides, generated from the phenols **12**, **13** and **14**, proceeded in a highly stereoselective fashion to give the coupling product **15**. Cleavage of the chiral auxiliary by simple hydrolysis gave three different subseries of α-phenoxyphenyl acetic acids, i.e., the ketophenol series (ArOH = **12**), the benzoxazolones (ArOH = **13**) and the benzisoxazolones (ArOH = **14**), typically with an enantiomeric excess greater than 96%.

Each type of phenol used for the coupling reaction was synthesized by the synthetic routes that allowed for the incorporation of various R_1, R_2 and R_3 groups in the indicated positions. In each case, the incorporation of the R_2 and R_3 group is generally made possible either by use of commercially available ortho-substituted phenols or by utilizing various reactions directed by the ortho phenolic hydroxyl group. For the preparation of ketophenol **12**, a regioselective acylation at the position para to the phenolic hydroxyl group of **16** was achieved using various R_1-substituted acids in neat triflic acid. Alternatively, the addition of Grignard agents R_1MgX to the formyl group of **17** at the para position followed

Scheme 1. General Synthetic Route to α-Aryloxyphenylacetic Acid Derivatives[a]

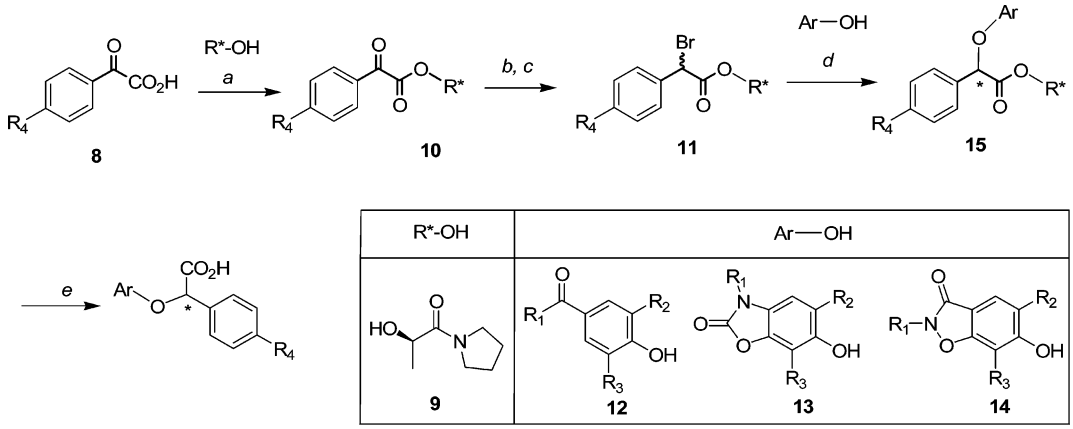

[a] Reagents and conditions: (a) $(COCl)_2$, then R*OH, Et_3N, CH_2Cl_2; (b) $NaBH_4$, THF; (c) PBr_3, CH_2Cl_2; (d) *t*-BuOLi, THF, 0 °C; (e) LiOH, H_2O_2 THF−H_2O.

Scheme 2. Synthesis of Phenols for the Ketone Series[a]

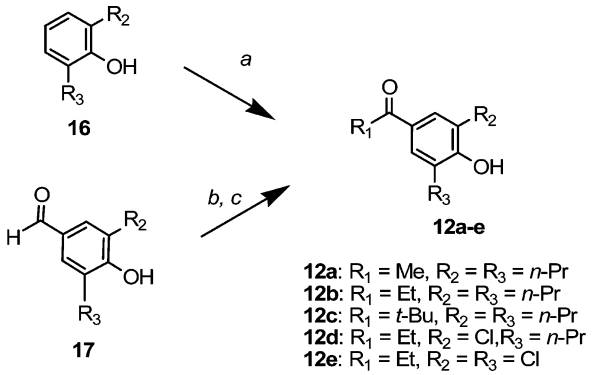

[a] Reagents: (a) R_1CO_2H, triflic acid, neat; (b) R_1MgX, THF; (c) TPAP/NMO, 4 Å MS, CH_2Cl_2.

Scheme 3. Synthesis of Phenols for the Benzoxazolone Series[a]

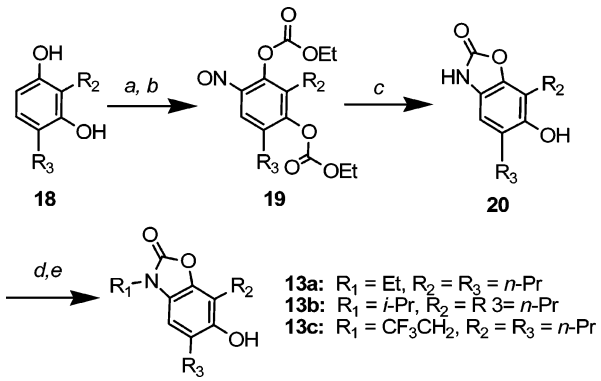

[a] Reagents and conditions: (a) $NaNO_2$, AcOH; (b) EtOCOCl, Et_3N, CH_2Cl_2; (c) H_2, Pd/C; (d) R_1-I, Cs_2CO_3; (e) NaOH, MeOH.

by oxidation has been used for the attachment of the R_1 group (Scheme 2).

The construction of the benzoxazolones **13** started with the nitrosation of R_2,R_3-substituted resorcinol **18** followed by reductive cyclization of the nitroso compound **19** to give cyclic intermediate **20**. Subsequent N-alkylation with various alkyl halides allowed the introduction of various R_1 groups (Scheme 3).

To prepare the benzisoxazolone phenol **14**, we have developed a novel method based on the use of the Mitsunobu reagent for cyclization of *o*-hydroxybenzohydroxamic acid **22**.[37] Compounds **22** were readily prepared from the corresponding hydroxybenzoic acids **21** and various R_1-substituted hydroxyamines (Scheme 4).

Results and Discussion

In Vitro SAR Studies. Compounds were evaluated for in vitro potency and subtype selectivity in PPAR scintillation proximity assays (SPA) and expressed as IC_{50} for displacement of a radiolabeled reference compound. Their agonist responses were measured in the cell-based transactivation assay (TA) using PPAR-GAL4 chimeric receptors and a reporter gene containing a GAL-4 response element, and expressed as EC_{50}, defined as the concentration of test compound to produce 50% of maximal reporter activity. The maximal activity of a given compound was measured against that of a reference full agonist, being defined as 100%.

Since compound **5** itself was not suitable for in vivo studies due to the presence of an easily hydrolyzable

Scheme 4. Synthesis of Phenols for the Benzisoxazolone Series[a]

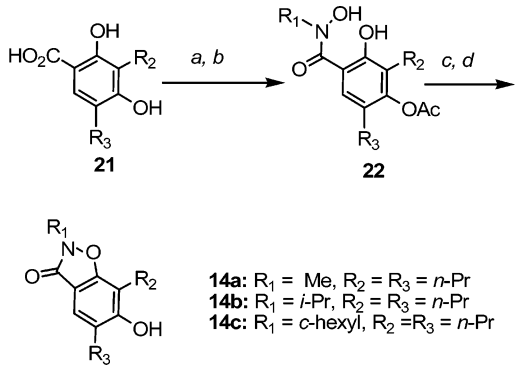

[a] Reagents and conditions: (a) AcCl, pyridine; (b) $(COCl)_2$, then R_1NHOH; (c) DEAD, Ph_3P, THF; (d) NaOH, MeOH−H_2O.

ester group (the corresponding diacid was completely inactive on PPAR α/γ receptors), our SAR studies began with the search for surrogates of the ester group in **5**. To this end, a variety of functional groups have been chosen to try to mimic the ester group (Chart 3). However, our initial attempt met with only limited success. Thus, the replacement of the ester group with an amide, a sulfone or a lactone moiety (compounds **23**, **26**, **27**) led to the complete loss of activity. The relocation of the ester group from para to meta position (compound **24**) also abolished the activity. The substitution of a *gem*-difluoropropyl group for the methyl ester (compound **25**) retained much of the binding potency but suffered a considerable loss of activity in transactivation assay, suggesting that the presence of a carbonyl group in this region is required for maintaining functional activity. Fortunately, an ethylcarbonyl group was found to be able to imitate the original ester group to give compound **28**, which maintained the same binding affinities for both α and γ receptors as those of compound **5**.

With the successful replacement of a ketone for the ester residue, the structure−activity relationships involving the R_1−R_4 groups on the ketone-based scaffold were investigated in more detail (Table 1). In general, it was found that most active analogues in this series have inherited the unique in vitro profile of the lead compound **5**, such that they all behaved as "super agonists" for PPARα and as weak or partial agonists for PPARγ in transactivation assays despite of having comparable binding affinities for both α and γ receptors. With regard to the R_1 group, several lipophilic alkyl groups, but not aryls (compound **31**), seemed to be well tolerated, though they did not offer any advantage over the ethyl group in terms of pharmacokinetic properties or in vivo efficacy. On the other hand, quite restrictive SAR was seen for the R_2 and R_3 groups attached to both sides of the phenoxy ring. Thus, operations involving the removal of the two *n*-propyl groups or the substitution of one or both of the *n*-propyl groups with other alkyls or halogens resulted in complete or significant loss of binding activity (**32**−**36**), indicating that there are distinct structural requirements for the two *n*-propyl group to be present at both positions. Most notably, the installation of a lipophilic group at the R_4 position clearly increases the affinity for PPARγ receptor, but not on the PPARα (e.g. compound **28** vs **38**). To have

Chart 3. The Search for Ester Surrogates

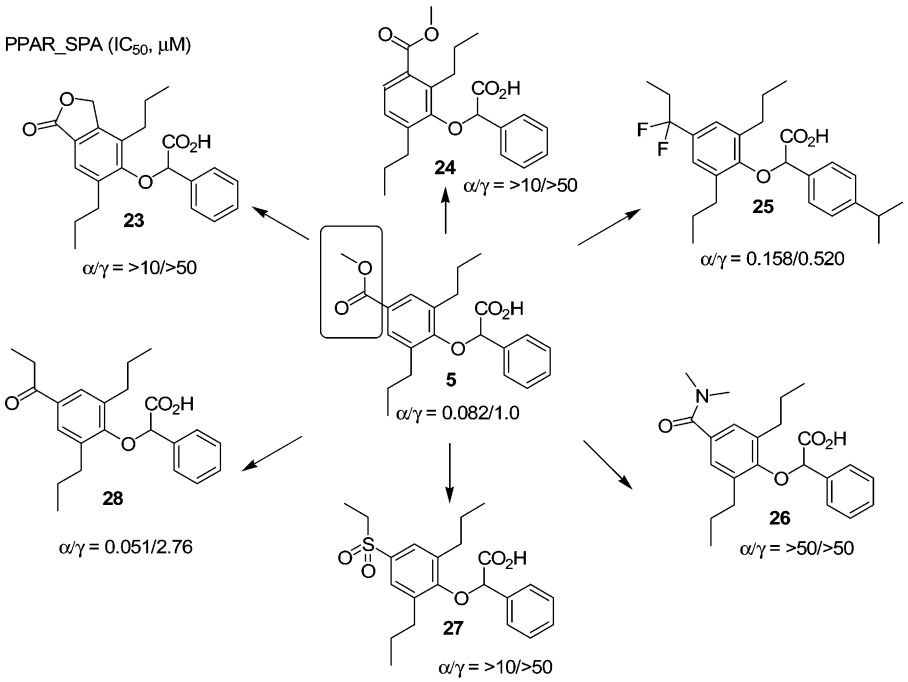

Table 1. In Vitro Human PPAR Activity of α-(*p*-Ketophenoxy)phenylacetic Acid

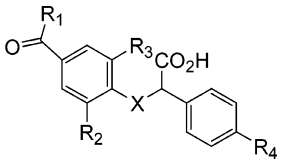

							binding IC_{50} (μM)[a]		TA EC_{50} (μM) (max %)[b]	
compd	*R*/*S*	X	R_1	R_2	R_3	R_4	PPARα	PPARγ	hPPARα	hPPARγ
28	racemic	O	Et	*n*-Pr	*n*-Pr	H	0.051	2.76	0.10 (1233%)	(28%)
29	racemic	O	*i*-Pr	*n*-Pr	*n*-Pr	H	0.16	3.16	0.25 (1650%)	(32%)
30	racemic	O	*t*-Bu	*n*-Pr	*n*-Pr	H	0.13	2.7	0.16 (1455%)	(53%)
31	racemic	O	Ph	*n*-Pr	*n*-Pr	H	0.80	4.68	–	–
32	racemic	O	Et	H	H	H	>50	>50	–	–
33	racemic	O	Et	s-Bu	s-Bu	H	6.12	>50	–	–
34	racemic	O	Et	Me	Me	H	3.0	>50	–	–
35	racemic	O	Et	Cl	Cl	H	1.6	>50	–	–
36	racemic	O	Et	Me	*n*-Pr	*i*-Pr	0.16	0.26	0.16 (810%)	0.197 (70%)
37	*S*	O	Et	Cl	*n*-Pr	*i*-Pr	0.26	0.22	0.26 (1138%)	0.36 (77%)
38	*S*	O	Et	*n*-Pr	*n*-Pr	Et	0.064	0.21	0.076 (675%)	0.48 (40%)
39	*S*	O	Et	*n*-Pr	n-Pr	*i*-Bu	0.058	0.22	0.039 (807%)	0.18 (66%)
40	*S*	O	Et	*n*-Pr	*n*-Pr	*i*-Pr	0.023	0.075	0.056 (1067%)	0.15 (50%)
41	*R*	O	Et	*n*-Pr	n-Pr	*i*-Pr	3.90	2.98	–	–
42	*S*	O	Et	*n*-Pr	n-Pr	i-PrO	0.043	0.20	0.11 (479%)	(59%)
43	*S*	O	Et	*n*-Pr	n-Pr	CF_3	0.089	0.21	0.25 (1448%)	(56%)
44	racemic	CH_2	Et	*n*-Pr	n-Pr	*i*-Pr	>15	>50	–	–
45	racemic	NH	Et	n-Pr	n-Pr	i-Pr	>50	>50	–	–

[a] Mean value of three determinations using scintillation proximity assay (SPA). [b] TA (transactivation assay). Mean value of three determinations. EC_{50}s were not calculated for compounds whose activity did not reach plateau at the maximal concentration of 3 μM; instead their percentage responses at a concentration of 3 μM were listed.

more balanced PPARα/γ activity, an isopropyl group was chosen as the optimized R_4 group since it imparts the best PPARγ activity without sacrificing PPARα activity

The effect of the stereochemistry at the α-position of the carboxylic acid was next examined. The opposite enantiomer of the isopropyl analogue **40**, one of the most active compounds in the series, was prepared according to Scheme 1 using the *S*-enantiomer of compound **9** as chiral auxiliary. The absolute configuration of each enantiomer was deduced based on mechanistic consideration[36] and was further confirmed in the X-ray cocrystal structure with PPAR-LBD (vide infra). The binding activities of the two enantiomers were compared. The results clearly showed that the binding affinity for both α and γ receptor mainly resided in the *S* enanantiomer, while the corresponding *R* enantiomer, compound **41**, was 160-fold and 40-fold less potent on PPARα and PPARγ, respectively. It should be noted that none of the analogues described here demonstrated significant binding to the PPARδ receptor (IC_{50} > 15 μM).

Scheme 5. Mechanism for Photoinduced Decomposition of Compound **40**

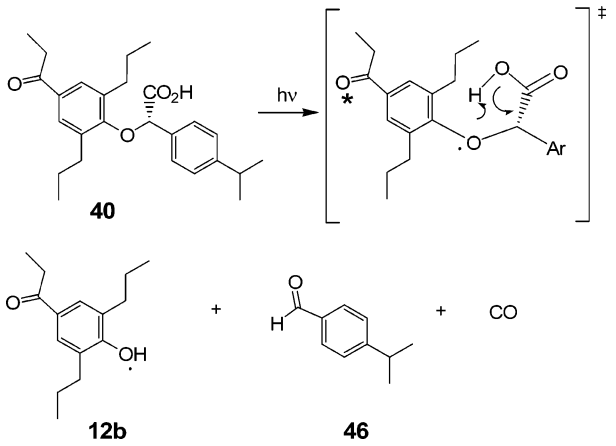

In the ketone series, compound **40** appeared to have the best overall in vitro profile and more consistent activity on human and murine PPAR receptors. It was also one of the most efficacious compounds in our in vivo models for glucose and lipid lowering (vide infra). However, during preclinical evaluation of **40**, we noticed that in an aqueous solution it showed some noticeable decomposition after being stored under ordinary laboratory light for 2 weeks. Since the decomposition occurred only under light and the product consisted mainly of the phenol **12b** and aldehyde **46**, we believed that the photoinduced fragmentation at the relatively weak benzylic ether bond was caused by the presence of the keto group at the para position which could well serve as sensitizer for photo activation (Scheme 5).[38]

To minimize the photoinstability problem, our first approach was to replace the ether linkage with a more robust bond such as a carbon−carbon or a carbon−nitrogen bond. Unfortunately and somewhat surprisingly, none of them was able to imitate the role of the C−O bond and the corresponding carbo analogue **44** (X = CH_2) and nitrogen analogue **45** (X = NH) were found to be devoid of PPAR activity. Thus the benzylic ether linkage in the current class of compounds appeared be essential for PPAR binding activity.

Our next approach to deal with the stability problem was to eliminate the photosensitizing keto group in the ketone series. Given that ketone appeared to be the only suitable surrogate for the ester residue among several promising noncyclic structural candidates, as described previously in Chart 3, our next effort was focused on the use of some cyclic structures as possible replacements for the ketone moiety. Gratifyingly, we have found that two alkyl substituted heterocyclic motifs,i.e., oxazolones and isoxazolones, when fused into the aromatic ring, could mimic efficiently the alkyl ketone moiety (Chart 4).

Table 2 details the SAR study that led to the optimization of compound **6** and **7**. The R_1 substituent on the nitrogen of each heterocyclic scaffold was investigated while keeping the R_2, R_3 and R_4 groups the same as those optimized in the ketone series. The data suggested that a lipophilic alkyl group at the R_1 position was well tolerated in the benzoxazolone series, though there was little to be gained from the additional steric bulk (**6**, **47**−**51**). On the other hand, increasing the size of R_1 significantly eroded the binding activity in the benzisoxazolone case (**56** and **57**), and a methyl group was found to be the best on both PPARα and γ (**7**). The structure−activity relationships regarding the R_2, R_3 and R_4 groups on the two heterocyclic scaffolds were found to be very much the same as those found in the ketone series. Thus, the replacement of the *n*-propyl group at R_3 with chlorine or removal of the alkyl group at R_4 reduced significantly the binding activity. Like the ketone analogues, compounds in these two heterocyclic series also exhibited "super" agonist activity for PPARα and weak or partial agonist activity for PPARγ. On the basis of their overall in vitro profiles, compound **6** and **7**, each representing the oxazolone and isoxazolone analogues, were chosen for further in vivo evaluation.

Chart 4. From Ketones to Benzoxazolones and Benzisoxazolones

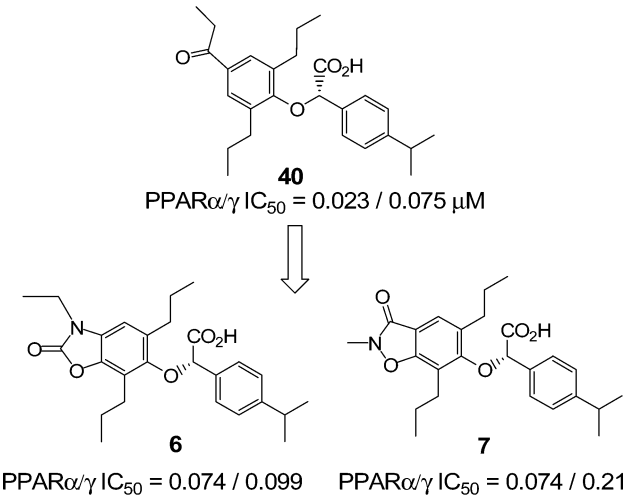

X-ray Crystallography Studies. One of the interesting features displayed by the current class of compounds is that they all showed weak or partial agonist response toward the hPPARγ receptor despite their relatively high binding affinity for the receptor and, as a indication of good cell permeability, a good match of potency in binding and transactivation assays. To further understand this interesting phenomenon, compound **7** was chosen to cocrystallize with PPARγ-LDB (residues Gln203 to Tyr477) as a binary complex without coactivator/corepressor peptides. In this crystal form, there were two PPARγ molecules in the crystallographic asymmetric unit, one in the activated conformation and one in an unactivated conformation. The structure was solved at a nominal resolution of 2.50 Å with an *R*-factor of 24.4% and *R*-free of 30.2%. There was clear electron density for compound **7** in the activated molecule, but the inactivated binding site was empty. For the purpose of comparison, the structure obtained was superimposed on the cocrystal structure of rosiglitazone with PPARγ-LBD, as shown in Figure 1. Compound **7** binds to the activated receptor with its carboxyl group forming a hydrogen bonding network involving Ser289 (helix 3), His323 (helix 6), His449 (helix 11) and Tyr473 (helix12). The isoxazolone ring sits in a hydrophobic pocket bounded by Ile281, Phe282, Cys285, Phe363 and Met364 in PPARγ. This site leads into a larger chamber in PPARγ which has been seen to accommodate groups the size of benzophenone (data unpublished). The *p*-isopropyl-substituted aromatic ring on **7** points along the path that wraps around behind

Table 2. In Vitro Human PPAR Activity of Benzoxazolone and Benzisoxazolone Analogues

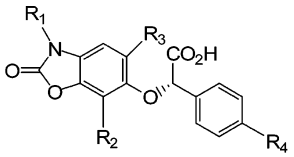

oxazolones (OXZ)

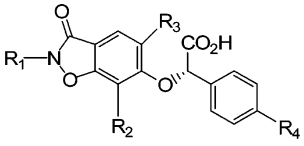

isoxazolones (IXZ)

						IC$_{50}$ (μM)		EC$_{50}$ (μM) (max %)	
compd	ring	R_1	R_2	R_3	R_4	PPARα	PPARγ	hPPARα	hPPARγ
47	oxz	CH_3	*n*-Pr	*n*-Pr	*i*-Pr	0.393	0.085	(680%)	0.64 (42%)
6	oxz	CH_3CH_2	*n*-Pr	*n*-Pr	*i*-Pr	0.074	0.099	0.29 (440%)	0.12 (36%)
48	oxz	$CH_3CH_2CH_2$	*n*-Pr	*n*-Pr	*i*-Pr	0.15	0.087	(218%)	0.12 (54%)
49	oxz	$(CH_3)_2CH$	*n*-Pr	*n*-Pr	*i*-Pr	0.072	0.051	0.14 (508%)	0.14(38%)
50	oxz	cyclopropylmethyl	*n*-Pr	*n*-Pr	*i*-Pr	0.13	0.12	(63%)	0.33 (36%)
51	oxz	CF_3CH_2	*n*-Pr	*n*-Pr	*i*-Pr	0.10	0.11	0.31 (123%)	0.14 (38%)
52	oxz	*i*-Pr	*n*-Pr	*n*-Pr	H	0.55	1.79	(1221%)	(27%)
53	oxz	CH_3CH_2	*n*-Pr	*n*-Pr	Cl	0.26	0.22	(861%)	(57%)
54	oxz	CH_3CH_2	*n*-Pr	Cl	*i*-Pr	1.41	0.52	(571%)	0.36 (48%)
55	ixz	CH_3	*n*-Pr	*n*-Pr	H	0.85	3.8	0.67 (1005%)	0.39 (41%)
7	ixz	CH_3	*n*-Pr	*n*-Pr	*i*-Pr	0.074	0.21	0.67 (1005%)	0.39 (41%)
56	ixz	$(CH_3)_2CH$	*n*-Pr	*n*-Pr	*i*-Pr	0.23	0.16	0.27 (889%)	0.43 (38%)
57	ixz	cyclohexyl	*n*-Pr	*n*-Pr	*i*-Pr	>15	0.44	(20%)	(23%)
58	ixz	*i*-Pr	n-*Pr*	n-*Pr*	i-*Bu*	0.79	0.26	(382%)	0.37 (35%)

[a] Mean value of three determinations using scintillation proximity assay (SPA). [b] TA (transactivation assay). Mean value of three determinations. EC$_{50}$s were not calculated for compounds whose activity did not reach plateau at the maximal concentration of 3 μM; instead their percentage responses at a concentration of 3 μM were listed.

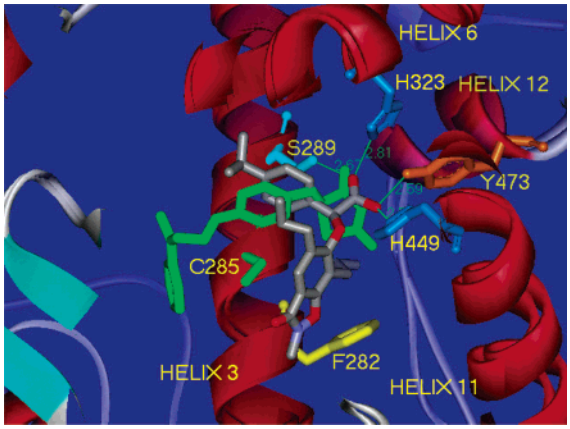

Figure 1. Superimposed crystal structures of the PPARγ-LBD in complex with compound **7** (grey) and rosiglitazone (green). Protein is depicted as red helices, cyan beta sheet and white random coil or turns. All residues within 3 Å of the ligand are shown.

helix 3, used by nearly all of the agonists whose complex structures have been solved.[27,39−41] However, unlike rosiglitazone, no part of **7** extends past the Cys285/Met364 boundary. Overall, these results suggested that simply forming a direct link to helix 12, although necessary, is not sufficient for full agonism. There may be some other aspect of compound **7**, such as compound size, shape and position in the ligand binding pocket that is unable to affect PPARγ in the same manner as rosiglitazone.

Although we do not have the corresponding structure of compound **7** with the PPARα receptor at this moment, it can be certain that compound **7** will also bind to the PPARα receptor in somewhat different fashion from a typical full agonist because of its relatively compact structure. In this context, the interesting question of why its interaction with the α receptor elicited an unusually higher agonist response in the PPARα-GAL4 transactivation assay remains to be answered.

Table 3. Pharmacokinetic Properties of Compound **40**, **6** and **7**

compds	species	bioavailability (%)	AUC[a] (μM h)	$t_{1/2}$ (h)[b]
40	rat	65	153.7	6.1
	dog	85	70.5	2.5
6	rat	72	127.2	6.0
	dog	35	9.1	1.2
7	rat	73	67.5	7.2
	dog	73	26.9	1.6

[a] Dosed at 2 mg/kg po. [b] Dose 0.5 mg/kg iv. See Experimental Section for details.

Pharmacokinetic and in Vivo Studies. Three representative compounds (**40**, **6**, and **7**) have been chosen for extensive in vivo evaluation. First, their pharmacokinectic parameters were examined in rats and dogs. As shown in Table 3, when dosed orally, all three compounds exhibited good exposure with excellent bioavailability and a good half-life.

Next, the in vivo pharmacology of compounds **6** and **7** was studied in a well-established rodent model of diabetes, using male *db/db* mice (10−11 week-old C57BLKS/J−m +/+*Lepr^{db}* mice), which is characterized by severe insulin resistance, hyperglycemia and marked hyper-triglyceridemia. As depicted in Figure 2, when dosed orally at 3 and 10 mg/kg by gavage once daily for 11 days, the two compounds demonstrated robust dose-related serum glucose-lowering efficacy (−69%, −95% for **6** at 3, 10 mpk and −58% for **7** at 10 mpk) that is either superior or comparable to the marketed PPARγ agonist rosiglitazone dosed at 10 mg/kg (−70% glucose reduction). As described above, both compounds **6** and **7** had PPARγ binding potency similar to that of rosiglitazone (PPARγ IC$_{50}$ $\sim$ 0.20 μM) but weaker agonist responses in the transactivation assay. Although it is not clear what fraction of the observed antihyperglycemic activity of these compounds is contributed by their PPARγ activity, the present results and the recent report of PPARα-mediated insulin sensitization[19,20] sug-

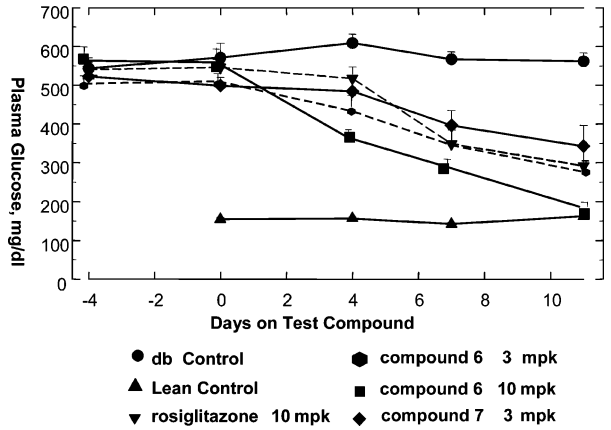

Figure 2. Effects of test compound on plasma glucose levels in *db*/*db* mice. Male *db*/*db* mice and lean mice were dosed daily for 11 days by gavage with vehicle or the indicated doses of test compounds. Each data point represents the mean value (±SD) of seven individual mice. Data for compound **6** at 3 mpk were taken from a separate study.

Table 4. Effects of Compounds **40**, **6** and **7** on Serum Cholesterol and Triglyceride in Hamster[a]

compd	dose (mpk)	cholesterol (mg/dL)[b]	change (%)[c]	TG (mg/dL)[b]	change (%)[c]
vehicle		128		331	
fenofibrate	100	91	−29	244	−26
40	3	88	−32	259	−22
40	10	86	−33	236	−29
6[d]	10	−	−25	−	−6
7	10	106	−17	303	−9

[a] Male Golden Syrian hamsters fed a normal rodent chow were orally dosed for 9 days with the test compounds. See Experimental Section for details. [b] Mean value ($n = 10$). [c] $p < 0.01$ vs vehicle control. [d] The data for this compound is obtained from a separate study where fenofibrate at 100 mpk showed −41% and −23% reductions in cholesterol and TG, respectively.

gest that a dual PPARα/γ agonist can provide better glucose control than currently marketed selective PPARγ agents.

To determine the ability of the current class of compounds to impact lipid homeostasis, male Syrian hamster and male Beagle dogs were used to investigate the effects of compounds **40**, **6** and **7** on the serum levels of triglyceride and total cholesterol. The former preclinical animal model faithfully predicts the clinical lipid modulating efficacy of fibric acid derivatives and the latter of fibric acid derivatives and statins.[42] As shown in Table 4, when administered orally to hamsters ($N = 6$) daily for 14 days compound **40** achieved superior cholesterol and triglyceride lowering compared to fenofibrate even at significantly lower dose. The apparent lack of dose response regarding the cholesterol reduction by **40** may suggest either a saturation of the response or a similar drug exposure at two doses. Further pharmacokinetic measurement should help to clarify this**.** The less robust lipid decrease by compound **6** and **7** may partly be due to their less potent hamster PPARα activity (**6**: $EC_{50} = 0.96\ \mu M$; **7**: $EC_{50} = 0.45\ \mu M$) compared with that of compound **40** ($EC_{50} = 0.085\ \mu M$). In male Beagle dogs, good lipid lowering efficacy was again achieved by both compound **40** and **7** (Table 5), though **40** was somewhat more potent ($EC_{50} = 0.13\ \mu M$) than **7** ($EC_{50} = 0.60\ \mu M$) in dog PPARα transactivation assay. It is worth noting that in the same dog model, the HMG CoA reductase inhibitor Simvastatin was able

Table 5. Effects of Compounds **40** and **7** on Serum Cholesterol in Dogs[a]

compound	dose (mpk)	change (%)[b]
fenofibrate	20	−4.7
fenofibrate	100	−23.5
40	10	−17.5
7	10	−17.3

[a] Male dogs being fed a normal chow diet were orally dosed daily with the test compounds at the indicated doses for 15 days. See Experimental Section for details. [b] Mean value ($n = 5$). [c] $p < 0.05$ vs vehicle control.

to lower cholesterol by 16% when dosed at 4 mg/kg.[42] These results clearly indicated that our PPARα/γ dual agonists can provide comparable cholesterol lowering efficacy to that achieved by fibrate drugs at much high doses or by statin drugs at similar dose levels.

To assess the typical PPARγ agonist-mediated side effects, compounds **6** and **7** were tested in a two week normal Sprague−Dawley (SD) rat tolerability study using the PPARγ full agonist rosiglitazone as a positive control. As shown in Table 6, the typical effects that include brown adipose tissue (BAT) proliferation, heart weight increases and hematocrit decrease were not seen with the current three compounds. The only major finding was an expected PPARα driven liver weight increase and some body weight decrease. In contrast, rosiglitazone increased heart weight by 22% and BAT depot mass 260% and decreased hematocrit by 12.5%. The lack of these PPARγ-related side effects with compounds **6** and **7** could well be due to the fact that these compounds possessed only partial PPARγ agonist activity, thereby raising the possibility that such agents may exert their PPARγ-mediated beneficial in vivo metabolic effects without provoking the undesirable side effects. Alternatively, the lack of PPARγ-mediated side effects may suggest that their in vivo pharmacology may have been largely driven by their PPARα activity.

Conclusion

In summary, we have described the synthesis and structure−activity studies of new series of α-aryloxyphenylacetic acid derivatives as a novel class of PPARα/γ dual agonists. Unlike most PPARα/γ dual agonists disclosed in the literature, these compounds are characterized by their balanced binding affinity for both PPARα and γ receptors along with a "super" agonist activity in PPARα−GAL4 TA assay and a weak or partial agonist activity toward PPARγ. The X-ray crystallographic analysis of cocrystal structures of PPARγ-LBD complexed respectively with compound **7** and rosiglitazone revealed a similarity as well as some significant differences in their interactions with the receptor. These differences were used to explain why most compounds described here elicited a partial agonist response toward PPARγ despite of their relatively high affinity for the receptor. Most notably, the three compounds chosen for in vivo evaluation demonstrated excellent anti-hyperglycemic efficacy in the *db*/*db* mouse and hypolipidemic activity in hamster and dog models, without provoking the typical PPARγ-mediate toxicity in rat tolerability model. These results suggest that further efforts to develop these novel PPARα/γ dual agonists as improved therapies for type 2 diabetes,

Table 6. PPARγ-Mediated Effects of Rosiglitazone and Compounds **6** and **7**

	vehicle	rosiglitazone	compound **6**	compound **7**
dose (mg/kg)	–	150	150	150
BAT (g)[b]	0.28 ± 0.05	**1.03 ± 0.32**	0.24 ± 0.04	0.24 ± 0.02
heart weight (g)[b]	1.19 ± 0.07	**1.46 ± 0.07**	1.10 ± 0.08	1.14 ± 0.08
liver weight (g)	15.0 ± 0.94	16.6 ± 1.66	**22.4 ± 3.13**	**20.3 ± 2.37**
hematocrit (%)[b]	47.2 ± 1.2	**41.3 ± 2.4**	45.6 ± 3.2	45.7 ± 2.6
body weight (g)[b]	321 ± 13	322 ± 13	**283 ± 19**	**278 ±13**

[a] Male normal rat fed a rodent chow with test compounds at the indicated doses for 2 weeks. For details, see the Experimental Section. [b] Mean value ± SD. Values in bold are those that are statistically different versus vehicle control.

dislipidemia and other aspects of metabolic syndrome are indeed warranted.

Experimental Section

In Vitro Assays. Activities of compounds were evaluated for both binding affinity and functional activity. First, binding affinities for the PPARs were measured in a scintillation proximity assay (SPA).[43] Second, potencies of PPAR gene activation were evaluated in cell-based transcription assays using GAL4-PPAR chimeric receptors as previous described.[44] All results were produced in triplicate, and mean values are reported. Generally, compound synthesis was driven by the SAR developed from these two assays.

In Vivo *db/db* Mouse Studies. *db/db* (C57BLKS/J−m +/+*Lepr*^{db}) mice were used as a type 2 diabetic animal model. Male *db/db* mice at 12−13 weeks of age and nondiabetic *db*/+ (lean) mice from Jackson Laboratories were housed seven mice per cage and fed a rodent chow (Purina no. 5001) ad libitum with free access to water. Mice (seven per group) received a once daily oral dosing of test compounds with vehicle (0.25% methylcellulose) by oral gavage for 11 days. Blood was collected from the tail immediately prior to the next dosing at days 0, 4, 7 and 11 for measurement of the plasma glucose levels.

Hamster Lipid Studies. Golden Syrian hamsters weighing between 120 and 150 g were purchased from Charles River Laboratories and used for the experiments. Hamsters were housed in boxes (five per box) and fed a normal rodent chow ad libitum with free access to water. Hamsters (10 for each group) were orally dosed with compounds (suspended in 0.5% methylcellulose) for 9 days. On the morning of the 10th day, hamsters were euthanized with carbon dioxide, and blood samples were obtained via heart puncture. Serum cholesterol and triglyceride levels were determined from the samples.

Dog Lipid Studies. Mature male Beagle dogs weighing between 12 and 18 kg were purchased from Marshall Farm, PA. They were housed individually and fed a cholesterol-free chow diet ad libitum with free access to water. Prior to starting experiments, the dogs (five for each group) were bled weekly from the jugular vein and their serum cholesterol levels were determined. Test compounds were suspended in 0.5% methylcellulose and gavaged daily to the dogs for 2 weeks. Blood samples were taken during and after the dosing periods, and serum cholesterol levels were determined.

Rat Tolerability Studies. Male Sprague−Dawley rats weighing about 200 g from Charles River were house 3 rats per cage and provided free access to water and rodent chow. Rats ($n = 6$) were orally dosed once daily by gavage with test compounds at indicated doses in 0.5% methylcellulose. Body weights were measured prior to each dosing on days 1, 4, 6 8, 11 and 14. Animals were euthanized via carbon dioxide 24 h following the last dose and the indicated tissue and organs were removed and weighed. Blood samples were drawn via heart puncture and assayed for serum chemistry.

Pharmacokinetic Studies. Male Sprague−Dawley rats ($n = 3$), male adult Beagle dogs ($n = 4$), and male adult Rhesus monkeys ($n = 3$) that had been fasted overnight received an oral gavage dose of 2 mg/kg, or an intravenous dose of 0.5 mg/kg by bolus injection. Blood samples were obtained from the femoral arterial cannula for rat, and the jugular vein for dog, at designated time points into heparin-containing tubes. The plasma was prepared immediately by centrifugation, acidified by the addition of 0.5 M formate buffer, pH 3.0, and stored at −70 °C. Quantitative analysis was carried out with LC-MS/MS using the PE Sciex API 3000 triplex quadruple mass spectrometer.

Synthetic Materials and Methods. Reagents and solvents were obtained from commercial suppliers and used without further purification. Flash chromatography was performed using E. Merck silica gel (230−400 mesh). ^{1}H NMR nuclear magnetic resonance (NMR) spectra were recorded in the deuterated solvents specified on a Varian Unity INOVA 500 MHz instrument. Chemical shifts are reported in ppm from the tetramethylsilane resonance in the indicated solvent (TMS: 0.0 ppm). The mass spectrum was measured using HP1100 and Micromass ZQ instruments (LC-MS system; a 4.6 × 50 mm RP-18 column and a gradient solvent system of 10−100% acetonitrile in water with 0.1% trifluoroacetic acid were used for HPLC and a positive electrospray ionization mode (ESI) for MS). Elemental analyses were obtained from Robertson Microlit Laboratories (Madison, NJ).

1-(4-Hydroxy-3,5-dipropylphenyl)propan-1-one (12b). A suspension of sodium propanoate (1.92 g, 20 mmol) and 2,6-di-propylphenol (1.78 g, 10 mmol) in neat triflic acid (10 mL) was heated at 50 °C for 1 h. The reaction mixture was poured into ice water and extracted with ethyl acetate (2 × 30 mL). The extract was washed with brine (2 × 30 mL) and aqueous sodium bicarbonate (30 mL), dried over $MgSO_4$ and concentrated. The residue was purified by chromatography on silica gel eluting with a 1:9 mixture of ethyl acetate:hexanes to give 1.98 g (85% yield) of **12b** as a white solid. ^{1}H NMR ($CDCl_3$, 500 MHz) δ 7.66 (s, 2H), 5.19 (br.s, 1H), 2.96 (q, $J = 7.3$ Hz, 2H), 2.62 (t, $J = 7.7$ Hz, 4H), 1.68 (m, 4H), 1.22 (t, $J = 7.3$ Hz, 3H), 1.01 (t, $J = 7.3$ Hz, 6H). MS (ESI) 235.11 (MH^+).

3-Ethyl-6-hydroxy-5,7-dipropyl-1,3-benzoxazol-2(3*H*)-one (13a). Step 1. Preparation of Ethyl 4-nitroso-2,6-dipropyl-1,3-phenylene Biscarbonate. To a solution of 2,6-dipropylresorsinol (9.7 g, 5.0 mmol) in acetic acid (50 mL) and ethanol (250 mL) cooled at −20 °C was added sodium nitrite (8.6 g, 125 mmol). The resulting suspension was stirred and warmed to room temperature overnight. The reaction mixture was diluted with ethyl acetate (500 mL) and washed successively with brine and a saturated solution of sodium bicarbonate. The organic phase was dried over $MgSO_4$ and filtered. The filtrate was treated with ethyl chloroformate (10.1 mL, 100 mmol) and triethylamine (22 mL, 150 mmol) at room temperature for 1 h and then concentrated to a small volume. The precipitated salt was removed, and the residue was purified by chromatography on silica gel eluting with a 8:2 mixture hexane:ethyl acetate to give 16.5 g (90% yield) of the title compound as a yellowish oil. ^{1}H NMR ($CDCl_3$, 400 MHz) δ 7.39 (s, 1H), 4.38 (m, 4H), 2.42−2.49 (m, 4H), 1.40−1.60 (m, 4H), 1.42 (t, $J = 7.5$ Hz, 3H), 1.41 (t, $J = 7.5$ Hz, 3H), 0.98 (t, $J = 7.5$ Hz, 3H), 0.95 (t, $J = 7.5$ Hz, 3H). MS (ESI) 368.31 (MH^+).

Step 2. 6-Hydroxy-5,7-dipropyl-1,3-benzoxazol-2(3*H*)-one. A solution of the product from Step 1 (16.5 g, 45 mmol) in ethyl acetate (250 mL) and 10% palladium on carbon (1.7 g) was stirred under hydrogen (1 atm) for 16 h. The reaction mixture was filtered through a pad of Celite, and the filtrate was concentrated. The residue was dissolved in DMF (250 mL) and stirred at 25 °C with Cs_2CO_3 (15 g, 45 mmol) for 4 h. The mixture was poured into water and extracted with ethyl acetate. The organic phase was washed with water, dried over $MgSO_4$ and concentrated. The residue was subjected to chro-

matography on silica gel eluting with a 7:3 mixture of hexane:ethyl acetate to give 9.0 g (80% yield) of the title compound as a solid. ^{1}H NMR ($CDCl_3$, 400 MHz) δ 8.70 (br.s, 1H), 6.70 (s, 1H), 4.60 (s, 1H), 2.78 (t, J = 7.5 Hz, 2H), 2.60 (t, J = 7.5 Hz, 2H), 1.50−1.70 (m, 4H), 0.99 (t, J = 7.5 Hz, 3H), 0.97 (t, J = 7.5 Hz, 3H). MS (ESI) 236.30 (MH^+).

Step 3. 3-Ethyl-6-hydroxy-5,7-dipropyl-1,3-benzoxazol-2(3*H*)-one (13a). To a solution of the product from Step 2 (8.2 g, 35 mmol) and pyridine (4.2 mL) in dichloromethane (150 mL) cooled at −30 °C was added dropwise acetyl chloride (2.6 mL, 36.5 mmol). The reaction was warmed to room temperature over 1 h and poured into 0.5 N hydrochloric acid. The organic phase was separated, washed with brine, dried over $MgSO_4$ and concentrated. The residue was dissolved in DMF (150 mL) and stirred with Cs_2CO_3 (15 g, 46.5 mmol) at room temperature for 30 min. Ethyl iodide (5.6 mL, 70 mmol) was added, and stirring was continued for additional 1 h. The mixture was poured into water and extracted with ethyl acetate. The organic phase was washed with water, dried over $MgSO_4$ and concentrated. The residue was taken up in methanol (100 mL) and treated with 2 N KOH (20 mL) at room temperature for 30 min. The mixture was neutralized with concentrated hydrochloric acid and concentrated. The residue was purified by chromatography on silica gel eluting with a 8:2 mixture of hexane:ethyl acetate to give 6.9 g (75% yield) of the title product as a solid. ^{1}H NMR ($CDCl_3$, 500 MHz) δ 6.59 (s, 1H), 4.81(br.s, 1H), 3.82(q, J = 7.5 Hz, 2H), 2.77 (t, J = 7.5 Hz, 2H), 2.60 (t, J = 7.5 Hz, 2H), 1.60−1.70 (m, 4H), 1.36 (t, J = 7.5 Hz, 3H), 0.99 (t, J = 7.5 Hz, 3H), 0.95(t, J = 7.5 Hz, 3H). MS (ESI) 264.23 (MH^+).

6-Hydroxy-2-methyl-5,7-dipropyl-1,2-benzisoxazol-3(2*H*)-one (14a). Step 1. Preparation of Methyl 2,4-Dihydroxy-3,5-diallylbenzoate. Methyl 2,4-bis(allyloxy)-benzoate (37.2 g, 150 mmol), obtained from allylation of methyl 2,4-dihydroxybenzoate with allyl bromide, was dissolved in 1,2,4-trichlorobenzene (150 mL). The solution was heated under reflux for 7 h and then cooled to 25 °C. The reaction mixture was poured on the top of a column of silica gel and eluted first with hexane and then with 1:9 mixture of hexane: ethyl acetate to give 30 g (81%yield) of the title compound as an oil. ^{1}H NMR ($CDCl_3$, 400 MHz): 11.0 (s, 1H), 7.58 (s, 1H), 5.93−6.06 (m, 2H), 5.75 (s, 1H), 5.10−5.21 (m, 4H), 3.96 (s, 3H), 3.52 (m, 2H), 3.36 (m, 2H).

Step 2. Preparation of 2,4-Dihydroxy-3,5-dipropylbenzoic Acid. A solution of the product from Step 1 (30 g, 121 mmol) in ethyl acetate (500 mL) and palladium on carbon (10%, 1.5 g) was stirred under hydrogen (1 atm) for 6 h. The catalyst was filtered off through a pad of Celite, and the filtrate was concentrated. The residue was dissolved in methanol (500 mL) and treated with 3 N NaOH (80 mL) under reflux for 16 h. The reaction mixture was concentrated and the residual aqueous phase was neutralized with 2 N HCl to pH 2. The precipitated solid was collected by filtration, washed briefly with water and cold methanol, and dried under vacuum to give 24 g (83% yield) of the title compound as a white solid. ^{1}H NMR ($CDCl_3$, 400 MHz): 7.01 (s, 1H), 5.2 (s, 1H), 2.68 (t, J = 7.5 Hz, 2H), 2.52 (t, J = 7.5 Hz, 2H), 1.60−1.70 (m, 4H), 0.99 (t, J = 7.5 Hz, 3H), 0.96 (t, J = 7.5 Hz, 3H). MS (ESI) 239.20 (MH^+).

Step 3. *N*-Methyl-4-acetoxy-3,5-dipropyl-6-hydroxybenzohydroxamic Acid. The acid from Step 2 (24 g, 100 mmol) and acetyl chloride (21 mL, 300 mmol) were dissolved in dichloromethane (250 mL). Pyridine (35.0 mL, 432 mmol) was added dropwise at 0 °C. The reaction mixture was warmed to 25 °C over 1 h and poured into 0.5 N hydrochloric acid (250 mL). The separated organic layer was washed with brine, dried over $MgSO_4$ and concentrated. The residue was dissolved in dichloromethane (50 mL) and treated with oxalyl chloride (16.4 mL, 200 mmol) and 2 drops of DMF under reflux for 1 h. All the volatiles were then removed by azeotroping with toluene (2 × 50 mL). The residue was redissolved in dichloromethane (400 mL) and added to a vigorously stirred biphasic mixture containing *N*-methylhydroxyamine hydrochloride (25 g, 300 mmol), diethyl ether (200 mL) and 2 N aqueous sodium carbonate (200 mL). After 30 min of vigorous stirring, the reaction mixture was acidified with 2 N hydrochloric acid to pH 2 and extracted with ethyl acetate. The organic layer was washed with brine, dried over $MgSO_4$ and concentrated. The residue was purified by chromatography on silica gel eluting with a 7:3 mixture of hexane:ethyl acetate to give 20 g (65% yield) of the title compound as a brown oil. ^{1}H NMR($CDCl_3$, 400 MHz): δ 7.05 (s, 1H), 3.59 (s, 3H), 2.46−2.60 (m, 2H), 2.30−2.41 (m, 2H), 2.38 (s, 3H), 1.41−1.56 (m, 4H), 0.98 (t, J = 7.2 Hz, 3H), 0.96 (t, J = 7.2 Hz, 3H). MS (ESI): 310.22 (MH^+).

Step 4. 6-Hydroxy-2-methyl-5,7-dipropyl-1,2-benzisoxazol-3(2*H*)-one (14a). The product from Step 3 (3.1 g, 10 mmol) and triphenylphosphine (3.9 g, 15 mmol) were dissolved in dry THF (100 mL). To the resulting solution was added dropwise diethyl azodicarboxylate (2.6 g, 15 mmol). After being stirred at 25 °C for 30 min, the mixture was quenched with a 1:1 mixture of methanol:acetic acid (1 mL) and concentrated. The residue was triturated with 1:1 hexane:diethyl ether and filtered through a pad of silica gel. The filtrate was concentrated, and the residue was dissolved in methanol (50 mL) and treated with 2 N NaOH (10 mL) for 30 min. The solution was neutralized with 2 N hydrochloric acid and evaporated to dryness under reduced pressure. The residue was purified by chromatography on silica gel eluting with a 7:3 mixture of hexane:ethyl acetate to give 2.1 g (86% yield) of the title compound. ^{1}H NMR ($CDCl_3$, 400 MHz): δ 7.43 (s, 1H), 6.50 (s, 1H), 0.3.63 (s, 3H), 2.77 (t, J = 7.1 Hz, 2H), 2.63 (t, J = 7.1 Hz, 2H), 1.65 (m, 4H), 0.99 (t, J = 7.5 Hz, 3H), 0.97 (t, J = 7.5 Hz, 3H). MS (ESI) 250.13 (MH^+).

Phenyl(4-propionyl-2,6-dipropylphenoxy)acetic Acid (28). A mixture of the phenol **12b** (1.7 g, 5.0 mmol), methyl α-bromophenylacetate (1.4 g, 6.0 mmol) and $CsCO_3$ (4.9 g, 7.5 mmol) in DMF (25 mL) was stirred at room temperature for 2 h. The reaction mixture was poured into water and extracted with ethyl acetate. The organic phase was washed with water, dried over $MgSO_4$ and concentrated. The residue was taken up in methanol (25 mL) and treated with 2 N NaOH (5 mL) for 30 min. The mixture was acidified with 2 N hydrochloric acid and concentrated under reduced pressure. The residue was purified by chromatography on silica gel eluting with a 7:3 mixture of hexane:ethyl acetate containing 0.1% acetic acid to give 1.56 g (85% yield) of compound **28**. ^{1}H NMR (CD_3OD, 500 MHz) δ 7.65 (s, 2H), 7.49 (m, 2H), 7.40 (m, 3H) 5.18 (s, 1H) 2.99 (q, 2H, J = 7.3 Hz), 2.44 (m, 4H), 1.51 (m, 4H) 1.15 (t, 3H, J = 7.3 Hz) 0.83 (t, 6H, J = 7.3 Hz). MS (ESI) 369.10 (MH^+).

(2*R*)-1-Oxo-1-pyrrolidin-1-ylpropan-2-ol (9). A mixture of isobutyl (*R*)-(+)-lactate (25 mL, 166 mmol) and pyrrolidine (27.7 mL, 332 mmol) were kept at 25 °C for 3 days. The volatiles was then removed in a rotavapor, and the residue was azeotroped with toluene (2 × 100 mL) to give essentially pure compound **5** as a brown oil. ^{1}H NMR ($CDCl_3$, 500 MHz) δ 4.90 (q, J = 6.9 Hz, 1H), 3.61−3.72 (m, 2H) 3.35−3.50 (m, 2H), 1.53 (m, 2H) 1.42 (m, 2H), 1.32 (d, J = 6.9 Hz, 3H).

(4-Isopropylphenyl)(oxo)acetic Acid (8, R_4 = *i*-Pr). At 0 °C, aluminum trichloride (26.7 g, 0.20 mmol) was added to a solution of isopropylbenzene (24.0 g, 0.20 mole) and ethyl chlorooxoacetate (41.0 g, 0.30 mol) in dichloromethane (0.50 L). The resulting mixture was stirred at 25 °C for 2 h and then poured into 0.5 N hydrochloric acid (0.50 L). The organic layer was separated, and the aqueous phase was extracted with dichloromethane (2 × 200 mL). The combined organic layers were washed successively with brine (300 mL) and saturated aqueous sodium bicarbonate (300 mL), dried over $MgSO_4$ and concentrated. The residue was taken up in methanol (500 mL) and treated with 2 N NaOH (83 mL) for 30 min. Methanol was removed under reduced pressure, and the remaining aqueous phase was extracted with diethyl ether and acidified with 2 N hydrochloric acid to pH 2. The precipitated product was collected, washed with water and air-dried to give 22 g of crude compound **8** (R = *i*-Pr). ^{1}H NMR ($CDCl_3$, 400 MHz) δ 8.1 (d, J = 8.0 Hz, 2H), 7.31 (d, J = 8.0 Hz, 2H), 3.20 (m, 1H), 1.25 (d, J = 7.2 Hz, 6H).

(1*R*)-1-Methyl-2-oxo-2-pyrrolidin-1-ylethyl (4-isopropylphenyl)(oxo)acetate (10, R_4 = *i*-Pr). A solution of the crude keto acid **8** (22.0 g) and oxalyl chloride (19.9 mL, 228 mmol) in dichloromethane (100 mL) was treated with 2 drops of DMF and refluxed for 30 min. All the volatiles were then distilled off, and the residue was azeotroped with toluene (100 mL) under reduced pressure. The residue (27.5 g) was mixed with the (*R*)-lactamide **9** (16.3 g, 114 mmol) in dichloromethane (200 mL) at 0 °C and treated with triethylamine (31.0 mL, 228 mmol). The reaction mixture was warmed to 25 °C over 30 min and poured into 0.5 N hydrochloric acid (300 mL). The organic layer was separated, and the aqueous phase was extracted with dichloromethane (100 mL). The combined organic phases were washed with brine, dried over $MgSO_4$ and concentrated. The residue was subjected to chromatography on silica gel eluting with a 1:1 mixture of hexane:ethyl acetate to give 28.9 g (80% yield) of compound **10** (R = *i*-Pr) as a white solid. ^{1}H NMR ($CDCl_3$, 400 MHz) δ 8.1 (d, J = 8.0 Hz, 2H), 7.31(d, J = 8.0 Hz, 2H), 5.39 (q, J = 7.0 Hz, 1H), 3.60−3.79 (m, 2H), 3.40−3.55 (m, 2H), 3.20 (m, 1H), 1.90−2.12 (m, 4H), 1.60 (d, J = 7.0 Hz. 3H), 1.26 (d, J = 7.2 Hz, 6H). MS (ESI) 318.20 (MH^+).

(1*R*)-1-Methyl-2-oxo-2-pyrrolidin-1-ylethyl Bromo(4-isopropylphenyl)acetate (11, R = *i*-Pr). To a solution of the keto ester **10** (R_4 = *i*-Pr, 5.08 g, 16.0 mmol) in dry THF (100 mL) cooled at 0 °C was added sodium borohydride (0.302 g, 8.0 mmol). The reaction mixture was stirred at 0 °C for 30 min and then poured into a cold mixture of brine (50 mL) and 2 N hydrochloric acid (4 mL). The organic layer was separated, and the aqueous phase was extracted with ethyl acetate. The combined organic layers were washed with brine, dried over $MgSO_4$ and concentrated. The residue (4.6 g) was dissolved in dichloromethane (50 mL) at 25 °C and treated with phosphorus tribromide (1.37 mL, 14.5 mmol) at 25 °C. After 30 min, the mixture was poured into brine (100 mL), and the separated organic phase was washed with brine, dried over $MgSO_4$ and concentrated. The residue was purified by chromatography on silica gel eluting with a 1:1 mixture of hexane:ethyl acetate to give 5.0 g (82% yield) of compound **11** (R = i-Pr) as a 1:1 mixture of diastereomers. ^{1}H NMR ($CDCl_3$, 500 MHz): δ? 7.50 (d, J = 8.5 Hz, 0.5 × 2 H), 7.49 (d, J = 8.5 Hz, 0.5 × 2 H), 7.20−7.26 (m, 2H), 5.42 (s, 1 H), 5.29 (q, J = 7.0 Hz, 0.5 × 1 H), 5.27 (q, J = 7.0 Hz, 0.5 × 1 H), 3.30−3.60 (m, 4H), 2.9 (m, 1 H), 1.80−2.0 (m, 4H), 1.50 (d, J = 7.0 Hz, 0.5 × 3H), 1.45 (d, J = 7.0 Hz, 0.5 × 3H), 1.25 (d, J = 7.2 Hz, 0.5 × 6 H), 1.24 (d, J = 7.2 Hz, 0.5 × 6H). MS (ESI) 382.30, 384.21 (MH^+).

General Procedure A: Coupling of the Bromide 11 with Phenols 12−14. To a solution of the phenol (5.0 mmol) in THF (50 mL) was added a solution of lithium *tert*-butoxide in THF (1.0 M, 4.8 mL, 4.8 mmol). The resulting solution was cooled to 0 °C, and a solution of the chiral bromide **11** (1.9 g, 5.0 mmol) in THF (5.0 mL) was added. The reaction mixture was stirred at 0 °C overnight, quenched with acetic acid (0.5 mL) and poured into water (50 mL). The organic phase was separated, and the aqueous phase was extracted with ethyl acetate (30 mL). The combined organic phase was washed with brine, dried over $MgSO_4$ and concentrated. The residue was purified by chromatography on silica gel using a mixture of hexane:ethyl acetate as the eluent.

(1*R*)-1-Methyl-2-oxo-2-pyrrolidin-1-ylethyl (2*S*)−(4-isopropylphenyl)(4-propionyl-2,6-dipropylphenoxy)-acetate (15a: R_4 = *i*-Pr; ArOH = 12b): 92% yield using compound **12b** as the phenol. ^{1}H NMR 500 MHz (CD_3OD); 7.64 (s, 2H), 7.39 (d, J = 8.0 Hz, 2H), 7.28 (d, J = 8.1 Hz, 2H) 5.32 (s, 1H), 5.27 (q, J = 6.9 Hz, 1H), 3.72 (m, 1H), 3.61 (m, 1H) 3.35−3.50 (m, 4H), 2.98 (q, J = 7.2 Hz, 2H), 2.93 (m, 1H) 2.41 (m, 4H), 1.93 (m, 2H) 1.86 (m, 3H) 1.53 (m, 2H) 1.42 (m, 2H), 1.32 (d, J = 6.9 Hz, 3H), 1.25 (d, J = 6.9 Hz, 6H), 1.15 (t, J = 7.3 Hz, 3H), 0.80 (t, J = 7.3 Hz, 6H). MS (ESI): 536.5 (MH^+).

(1*R*)-1-Methyl-2-oxo-2-pyrrolidin-1-ylethyl (2*S*)−(4-isopropylphenyl)[(3-ethyl-2-oxo-5,7-dipropyl-2,3-dihydro-1,3-benzoxazol-6-yl)oxy]acetate (15b: R_4 = *i*-Pr; ArOH = 13a): 95% yield using compound **13a** as the phenol. ^{1}H NMR (400 MHz, $CDCl_3$): δ 7.40 (d, J = 8.0 Hz, 2H), 7.18 (d, J = 8.0 Hz, 2H), 6.60 (s, 1H),5.29 (q, J = 7.5 Hz, 1H) 5.16 (s, 1H), 3.85 (q, J = 7.5 Hz, 2H), 3.52−3.63 (m, 2H), 3.45 (m, 1H), 3.35 (m, 1H), 2.98 (m, 1H), 2.35−2.56 (m, 4H) 1.82−2.0 (m, 4H), 1.40−1.60 (m, 4H), 1.38 (t, J = 7.5 Hz, 3H), 1.36 (d, J = 7.5 Hz, 3H), 1.28 (d, J = 7.5 Hz, 6H), 0.85 (t, J = 7.5 Hz, 3H), 0.78 (t, J = 7.5 Hz, 3H). MS (ESI): 565.7 (MH^+).

(1*R*)-1-Methyl-2-oxo-2-pyrrolidin-1-ylethyl (2*S*)-(4-isopropylphenyl)[(2-methyl-3-oxo-5,7-dipropyl-2,3-dihydro-1,2-benzisoxazol-6-yl)oxy]acetate (15c: R_4 = *i*-Pr; ArOH = 14a): 95% yield using compound **14a** as the phenol. ^{1}H NMR (400 MHz, $CDCl_3$): δ 7.45 (s, 1H), 7.40 (d, J = 7.5 Hz, 2H), 7.25 (d, J = 7.5 Hz, 2H), 5.28 (s, 1H), 5.27 (q, J = 7.1 Hz, 1H), 3.62 (s, 3H), 3.40−3.56 (m, 4H), 2.95 (m, 1 H), 2.36−2.54 (m, 4H), 1.82−1.95 (m, 4H), 1.40−1.60 (m, 5H) 1.37 (d, J = 7.1 Hz, 3H), 1.24 (d, J = 7.2 Hz, 6H), 0.83 (t, J = 7.5 Hz, 3H), 0.81(t, J = 7.5 Hz, 3H). MS (ESI) 551.4 (MH^+).

General Procedure B: Hydrolysis of the Coupling Products 15. The coupling product obtained by General Procedure A (3.3 mmol) in THF (5.0 mL) was added to a mixture of 1 N LiOH (6.9 mL, 6.9 mmol) and 30% hydrogen peroxide (5.0 mL) in THF (20 mL) cooled at 0 °C. The reaction mixture was stirred at 0 °C for 2 h and then acidified with 2 N hydrochloric acid to pH 2. The organic layer was separated, and the aqueous layer was extracted with ethyl acetate (30 mL). The combined organic phase was washed with a 2 N solution of Na_2SO_3, dried over $MgSO_4$ and concentrated. The residue was purified by chromatography on silica gel using a 3:7 mixture of ethyl acetate:hexanes containing 1% of acetic acid as the eluent. The enantiomeric purity was determined by HPLC using a Cyclobond 2000 column (4.6 × 250 mm) and a solvent system of methanol:acetonitrile:acetic acid (20: 80: 1) at a flow rate of 1.5 mL/min.

(2*S*)-(4-Isopropylphenyl)(4-propionyl-2,6-dipropylphenoxy)acetic acid (40): 92% yield and 96% ee from hydrolysis of compound **15a**. ^{1}H NMR (500 MHz, CD_3OD) δ 7.64 (s, 2H), 7.38 (d, J = 8.2 Hz, 2H), 7.27 (d, J = 8.2 Hz, 2H), 5.13 (s, 1H), 2.99 (q, J = 7.2 Hz, 2H), 2.92 (m, 1H) 2.38−2.50 (m, 4H), 1.38−1.60 (m, 4H), 1.26 (d, J = 6.8 Hz, 6H), 1.15 (t, J = 7.2 Hz, 3H), 0.82 (t, J = 7.3 Hz, 6H). MS (ESI): 411.20 (MH^+). Anal. ($C_{26}H_{34}O_4$) C, H.

(2*S*)-[(3-Ethyl-2-oxo-5,7-dipropyl-2,3-dihydro-1,3-benzoxazol-6-yl)oxy](4-isopropylphenyl)acetic acid (6): 90% yield and 97% ee from hydrolysis of compound **15b**. ^{1}H NMR (CD_3OD, 500 MHz): δ 7.38 (d, J = 8.5 Hz, 2H), 7.28 (d, J = 8.5 Hz, 2H), 6.84 (s,1H), 5.03 (s, 1H), 3.84 (q, J = 7.0 Hz, 2H), 2.95 (m, 1 H), 2.38−2.55 (m, 4H), 1.35−1.60 (m, 4H), 1.31 (t, J = 7.0 Hz, 3H), 1.26 (d, J = 7.5 Hz, 6H), 0.82 (t, J = 7.5 Hz, 3H), 0.80 (t, J = 7.5, 3H). MS (ESI) 440.24 (MH^+). Anal. ($C_{26}H_{33}NO_5$) C, H, N.

(2*S*)-(4-Isopropylphenyl)[(2-methyl-3-oxo-5,7-dipropyl-2,3-dihydro-1,2-benzisoxazol-6-yl)oxy]acetic acid (7): 93% yeild and 96% ee from hydrolysis of compound **15c**. ^{1}H NMR (CD_3OD, 500 MHz) δ 7.45 (d, J = 8.0 Hz, 2H), 7.43 (s, 1H), 7.40 (d, J = 8.0 Hz, 2H), 5.17 (s, 1H), 3.62 (s, 3H), 2.86 (m, 1 H), 2.36−2.50 (m, 4H), 1.34−1.58 (m, 4H), 1.24 (d, J = 7.2 Hz, 6H), 0.82 (t, J = 7.5 Hz, 3H), 0.81 (t, J = 7.5, 3H). MS (ESI) 426.21 (MH^+). Anal. ($C_{25}H_{31}NO_5$) C, H, N.

X-ray Crystallography. Purified PPARgamma-LBD (residues Gln203 to Tyr477) at 10−15 mg/mL was mixed with compound **7** at a 1.6:1 ratio of compound:protein on ice and allowed to stand at 4 °C overnight. Crystals were grown by vapor diffusion at room temperature in 2 μL "sitting" drops that contained equal volumes of the protein complex solution and a reservoir solution consisting of 100 mM Tris-HCl, pH 8.0, 0.65−0.90 M Na_3 citrate, 1 mM TCEP, against 0.5 to 1.0 mL reservoir solutions in a Cryschem MVD-24 crystallization tray. Crystals were transferred to 100 mM Tris-HCl, pH 8.0, 1.44 M Na_3 citrate, and 1 mM TCEP and vitrified by plunging the nylon-loop-captured crystals into liquid nitrogen. A crystal was put into a cold, −170 °C nitrogen gas stream generated by a CryoStream model 600 (Oxford Cryosystems Inc.) for the duration of the diffraction experiment. X-ray diffraction data were collected in-house on a Rigaku FR-D X-ray generator operating at 50 kV, 100 mA, 20% bias voltage with the Cu Kα

beam focused with Osmic mirrors ("purple" optics). The diffraction data were collected as a series of 540 0.5° rotation images using an ADSC Quantum 4R 2 × 2 CCD area detector mounted on a Crystal Logics goniometer. Exposure time was set to keep low resolution reflection overloads at a minimum without significantly impacting the quality of the high-resolution data. Data were measured from a single crystal exhibiting *C*2 symmetry to a resolution of 2.5 Å. Measured intensities were reduced and scaled with DENZO and SCALEPACK from the HKL suite[45] that yielded an average redundancy on measurements of approximately 5 and an R_{sym} of 0.077 (see Supporting Information). The structure was solved using the coordinates for a previously elucidated selenomethionine PPARγ−LBD complex (unpulished results). Following rigid-body refinement of the starting structure, compound **7** was incorporated between rounds of model building using CHAIN[46] or XTALVIEW[47] and refinement using CNX (version 2002 Accelrys, Inc.)[48,49] The coordinates may be found in the Protein Data Bank under ID code 1ZEO.

Acknowledgment. We gratefully acknowledge technical assistance from Margaret Wu, Neelam Sharma, John Ventre, Roger Meurer, Chhabi Biswas and the pharmacokinetic measurements by Dr. Kwan Leung and Raul Alvaro. We also thank Dr. Peter Meinke for helpful discussions and reviewing of the manuscript.

Supporting Information Available: Additional experimental data. This material is available free of charge via the Internet at http://pubs.acs.org.

References

(1) Issemann, I.; Green, S. Activation of a member of the steroid hormone receptor superfamily by peroxisome proliferators. *Nature* **1990**, *347*, 645−650.
(2) Mangelsdorf, D. J.; Evans, R. M. The RXR heterodimers and orphan receptors. *Cell* **1995**, *83*, 841−850.
(3) Willson, T. M.; Brown, P. T.; Sternbach, D. D.; Henke, B. R. The PPARs: From orphan receptors to drug discovery. *J. Med. Chem.* **2000**, *43*, 527−550.
(4) Kersten, S.; Desvergne, B.; Wahli, W. Roles of PPARs in health and disease. *Nature* **2000**, *405*, 421−424.
(5) Chawla A.; Repa, J. J.; Evans, R. M.; Mangelsdorf, D. J. Nuclear receptors and lipid physiology: opening the X-files. *Science* **2001**, *294*, 1866−1870.
(6) Berger, J. P.; Moller, D. E. The mechanisms of action of PPARs. *Annu. Rev. Med.* **2002**, *53*, 409−435.
(7) Knouff, C.; Auwerx, J. Peroxisome proliferator-activated receptor-gamma calls for activation in moderation: lessons from genetics and pharmacology. *Endocr. Rev.* **2004**, *25*, 899−918.
(8) Martin, G.; Schoonjans, K.; Staels, B.; Auwerx, J. PPARγ activators improve glucose homeostasis by stimulating fatty acid uptake in the adipocytes. *Atherosclerosis* **1998**, *137* (Suppl.), S75−S80.
(9) Rosen, E. D.; Spiegelman, B. M. PPARγ: a nuclear regulator of metabolism, differentiation, and cell growth. *J. Biol. Chem.* **2001**, *276*, 37731−37734.
(10) Lehmann, J. M.; Moore, L. B.; Smith-Oliver, T. A.; Wilkinson, W. O.; Willson, T. M.; Kliewer, S. A. An antidiabetic thiazolidinedione is a high affinity ligand for peroxisome proliferator-activated receptor (PPARγ). *J. Biol. Chem.* **1995**, *270*, 12953−12956.
(11) Hulin, B.; McCarthy, P. A.; Gibbs, E. M. The glitazone family of antidiabetic agents. *Curr. Pharm. Des.* **1996**, *2*, 85−102.
(12) Ibrahimi, A.; Teboul, L.; Gaillard, D.; Amri, E. Z.; Ailhaud, G.; Young, P.; Cawthorne, M. A.; Grimaldi, P. A. Evidence for a common mechanism of action for fatty acids and thiazolidinedione antidiabetic agents on gene expression in preadipose cells. *Mol. Pharmacol.* **1994**, *46*, 1070−1076.
(13) Torra, I. P.; Gervois, P.; Staels, B. Peroxisome Proliferator-Activated Receptor alpha in Metabolic Disease, Inflammation, Atherosclerosis and Aging. *Curr. Opin. Lipidol.* **1999**, *10*, 151−159.
(14) Frick, M. H.; Elo, O.; Haapa, K.; Heinonen, O. P.; Heinsalmi, P.; Helo, P.; Huttunen, J. K.; Kaitaniemi, P.; Koskinen, P.; Manninen, V.; Maenpaa, H.; Malkonen, M.; Manttari, M.; Norola, S.; Pasternack, A.; Pikkarainen, J.; Romo, M.; Sjoblom, T.; Nikkila, E. A. Helsinki Heart Study: Primary-Prevention Trial with Gemfibrozil in Middle-Aged Men with Dyslipidemia. *N. Engl. J. Med.* **1986**, *314*, 488.
(15) Rubins, H. B.; Robins, S. J.; Collins, D.; Fye, C. L.; Anderson, J. W.; Elam, M. B.; Faas, F. H.; Linares, E.; Shaefer, E. J.; Shectman, G.; Wilt, T. J.; Wittes, J. Gemfibrozil for the secondary prevention of coronary heart disease in men with low level of high-density lipoprotein cholesterol. *N. Engl. J. Med.* **1999**, *341*, 410−418.
(16) Robins, S. J.; Collins, D.; Wittes, J. T.; Papademetrious, V.; Deedwania, P.; Schaefer, E.; McNamara, J. R.; Kashyap, M. L.; Hershman, J. M.; Wexler, L. F.; Rubins, H. B. Relation of gemfibrozil treatment and lipid levels with major coronary events. *J. Am. Med. Assoc.* **2001**, *285*, 1585−1591.
(17) Diabetes Atherosclerosis Intervention Study Investigators. Effect of fenofibrate on progression of coronary-artery disease in type 2 diabetes: The Diabetes Atherosclerosis Intervention Study, a randomized study. *Lancet* **2001**, *357*, 905−910.
(18) Naderali, E. K.; Fatani, S.; Williams, G. Fenofibrate lowers adiposity and corrects metabolic abnormalities, but only partially restores endothelial function in dietary obese rats. *Atherosclerosis* **2004**, *177*, 307−312.
(19) Guerre-Millo, M, Gervois, P.; Raspe, E.; Madsen, L.; Poulain, P.; Derudas, B.; Herbert, J.; Winegar, D.; Willson, T.; Fruchart, J.; Staels, B. Peroxisome proliferator-activated receptor α activators improve insulin sensitivity and reduce adiposity. *J Biol. Chem.* **2000**, *275*, 16638−16642.
(20) Ye, J.; Doyle, P.; Iglesias, M.; Watson, D.; Cooney, G.; Kraegen, E. Peroxisome proliferator-activated receptor-α activation lowers muscle lipids and improves insulin sensitivity in high fat-fed rats. *Diabetes* **2001**, *50*, 411−417.
(21) Expert Panel on Detection, Evaluation and Treatment of High Blood Cholesterol in Adults. Executive summary of the third report of the National Cholesterol Education Program (NCEP) Expert Panel on Detection, Evaluation, and Treatment of High Blood Cholesterol in Adults (Adult Treatment Panel III). *J. Am. Med. Assoc.* **2001**, *285*, 2486−2497.
(22) Henke, B. R. Peroxisome Proliferator-Activated Receptor α/γ Dual Agonists for the Treatment of Type 2 Diabetes. *J. Med. Chem.* **2004**, *47*, 4118−4127.
(23) Henke, B. R.; Blanchard, S. G.; Brackeen, M. F.; Brown, K. K.; Cobb, J. E.; Collins, J. L.; Harrington, W. W., Jr.; Hashim, M. A.; Hull-Ryde, E. A.; Kaldor, I.; Kliewer, S. A.; Lake, D. H.; Leesnitzer, L. M.; Lehmann, J. M.; Lenhard, J. M.; Orband-Miller, L. A.; Miller, J. F.; Mook, R. A.; Noble, S. A.; Oliver, W.; Parks, D. J.; Plunket, K. D.; Szewczyk, J. R.; Willson, T. M. (2-Benzoylphenyl)-L-tyrosine PPARγ Agonists. 1. Discovery of a Novel Series of Potent Antihyperglycemic and Antihyperlipidemic Agents. *J. Med. Chem.* **1998**, *41*, 5020.
(24) Murakami, K.; Tobe, K.; Ide, T.; Mochizuki, T.; Ohashi, M.; Akanuma, Y.; Yazaki, Y.; Kadowaki, T. A novel insulin sensitizer acts as coligand for peroxisome proliferator-activated receptor α (PPAR-α) and PPAR-γ: effect of PPAR-α activation on abnormal lipid metabolism in liver of Zucker fatty rat. *Diabetes* **1998**, *47*, 1841−1847.
(25) Lohray, B. B.; Lohray, V. B.; Bajji, A. C.; Kalchar, S.; Poondra, R. R.; Padakanti, S.; Chakrabarti, R.; Vikramadithyan, R. K.; Misra, P.; Juluri, S.; Mamidi, N. V. S. R.; Rajagopalan, R. (−)3-[4-[2-Phenoxazin-10-yl)ethoxy]phenyl]-2-ethoxypropanoic Acid-[(−)DRF2725]: A dual PPAR agonist with potent antihyperglycemic and lipid modulating activity. *J. Med. Chem.* **2001**, *44*, 2675−2678.
(26) Brooks, D. A.; Etgen, G. J.; Rito, C. J.; Shuker, A. J.; Dominianni, S. J.; Warshawsky, A. W.; Ardecky, R.; Paterniti, J. R.; Tyhonas, J.; Broderick, C. L.; Oldham, B. A.; Montrose-Rafizadeh, C.; Winneroski, L. L.; Faul, M. M.; McCarthy, J. R. Design and synthesis of 2-methyl-2-{4-[2-(5-methyl-2-aryloxazol-4-yl)ethoxy]-phenoxy}propionic acids: A new class of dual PPARα/γ agonists. *J. Med. Chem.* **2001**, *44*, 2061−2064.
(27) Sauerberg, P.; Pettersson, I.; Jeppesen, L.; Bury, P. S.; Morgensen, J. P.; Wassermann, K.; Brand, C. L.; Sturis, J.; Woldike, H. F.; Fleckner, J.; Andersen, A. T.; Mortensen, S. B.; Svensson, l. A.; Rasmussen, H. B.; Lehmann, S. V.; Polivka, Z.; Sindelar, K.; Panajotova, V.; Ynddal, L.; Wulff, E. M. Novel tricyclic-α-alkoxyphenylpropionic acids: Dual PPARα/γ agonists with hypolipidemic and antidiabetic Activity. *J. Med. Chem.* **2002**, *45*, 789−804.
(28) Cheng, P. T.; Chandrasena, G.; Chen, S. BMS-298585 is a novel, uniquely balanced dual activator of peroxisome proliferator-activated receptors (PPAR) alpha and gamma, with an excellent ADME profile. *Diabetes* **2002**, *51* (Suppl. 2), A94.
(29) Desai, R. C.; Gratale, D. F.; Han, W.; Koyama, H.; Metzger, E.; Lombardo, V. K.; MacNaul, K. L.; Doebber, T. W.; Berger, J. P.; Leung, K.; Franklin, R.; Moller, D. E.; Heck, J. V.; Sahoo, S. P. Aryloxazolidinediones: identification of potent orally active

PPAR dual α/γ agonists. *Bioorg. Med. Chem. Lett.* **2003**, *13*, 3541−3544.
(30) Desai, R. C.; Han, W.; Metzger, E. J.; Bergman, J. P.; Gratale, D. F.; MacNaul, K. L.; Berger, J. P.; Doebber, T. W.; Leung, K.; Moller, D. E.; Heck, J. V.; Sahoo, S. P. 5-Aryl thiazolidine-2,4-diones: discovery of PPAR dual α/γ agonists as antidiabetic agents, *Bioorg. Med. Chem. Lett.* **2003**, *13*, 2795−2798.
(31) Adams, A. D.; Hu, Z.; von Langen, D.; Dadiz, A.; Elbrecht, A.; MacNaul, K. L.; Berger, J. P.; Doebber, T. W.; Meurer, R.; Forrest, M. J.; Moller, D. E.; Jones, A. B. *O*-Arylmandelic acids as highly selective human PPARα/γ agonists. *Bioorg. Med. Chem. Lett.* **2003**, *13*, 3185−3190.
(32) Koyama, H.; Miller, D. J.; Boueres, J. K.; Desai, R. C.; Jones, A. B.; Berger, J. P.; MacNaul, K. L.; Kelly, L. J.; Doebber, T. W.; Wu, M. S.; Zhou, G.; Wang, P. R.; Ippolito, M. C.; Chao, Y. S.; Agrawal, A. K.; Franklin, R.; Heck, J. V.; Wright, S. D.; Moller, D. E.; Sahoo, S. P. (2R)-2-ethylchromane-2-carboxylic acids: discovery of novel PPARalpha/gamma dual agonists as antihyperglycemic and hypolipidemic agents. *J. Med. Chem.* **2004**, *47*, 3255−63.
(33) Devasthale, P. V.; Chen, S.; Jeon, Y.; Qu, F.; Shao, C.; Wang, W.; Zhang, H.; Cap, M.; Farrelly, D.; Golla, R.; Grover, G.; Harrity, T.; Ma, Z.; Moore, L.; Ren, J.; Seethala, R.; Cheng, L.; Sleph, P.; Sun, W.; Tieman, A.; Wetterau, J. R.; Doweyko, A.; Chandrasena, G.; Chang, S. Y.; Humphreys, W. G.; Sasseville, V. G.; Biller, S. A.; Ryono, D. E.; Selan, F.; Hariharan, N.; Cheng, P. T. W. Design and Synthesis of *N*-[(4-Methoxyphenoxy)-carbonyl]-*N*-[[4-[2-(5-methyl-2-phenyl-4-oxazolyl)ethoxy]phenyl]-methyl]glycine [Muraglitazar/BMS-298585], a Novel Peroxisome Proliferator-Activated Receptor α/γ Dual Agonist with Efficacious Glucose and Lipid-Lowering Activities. *J. Med. Chem.* **2004**, *48*, 2248−2250.
(34) Bristol-Myers Squibb Company Press Release: Bristol-Myers Squibb Provides Regulatory Update for Muraglitazar and Abatacept. December 23, 2004.
(35) The definition of the term "super" agonist is somewhat arbitrary. We use this term to characterize the compounds described in this paper whose maximal agonist responses in the cell-based transactivation assay are generally 3−20 times higher than a typical reference full agonist.
(36) Devine, P. N.; Dolling, U.-H.; Heid, R. M.; Tschaen, D. M. Stereoselective synthesis of 2-aryloxy acids from lactamide derived esters of racemic α-halo carboxylic acids. *Tetrahedron Lett.* **1996**, *37*, 2683−2686.
(37) Shi, G. The first general synthesis of *N*-substituted 1,2-benzisoxazolin-3-ones. *Tetrahedron Lett.* **2000**, *41*, 2295.
(38) Albini, A. Photosensitization in Organic Synthesis. *Synthesis*. **1981**, 249−264.
(39) Nolte, R. T.; Wisely, G. B.; Westin, S.; Cobb, J. E.; Lambert, M. H.; Kurokawa, R.; Rosenfeld, M. G.; Willson, T. M.; Glass, C. K.; Milburn, M. V. Ligand binding and co-activator assembly of the peroxisome proliferator-activated receptor-γ. *Nature* **1998**, *395*, 137−143.
(40) Xu, H. E.; Lambert, M. H.; Montana, V. G.; Plunket, K. D.; Moore, L. B.; Collins, J. L.; Oplinger, J. A.; Kliewer, S. A.; Gampe, R. T., Jr.; McKee, D. D.; Moore, J. T.; Willson, T. M. Structural determinants of ligand binding selectivity between the peroxisome proliferator-activated receptors. *Proc. Natl. Acad. Sci. U.S.A.* **2001**, *98*, 13919−13924.
(41) Cronet, P.; Petersen, J. F.; Folmer, R.; Blomberg, N.; Sjoblom, K.; Karlsson, U.; Lindstedt, E. L.; Bamberg, K. Structure of the PPARalpha and -gamma ligand binding domain in complex with AZ 242; ligand selectivity and agonist activation in the PPAR family. *Structure* **2001**, *9*, 699−706.
(42) Chao, Y. S.; et al. Unpublished results.
(43) Berger, J. P.; Petro, A. E.; Macnaul, K. L.; Kelly, L. J.; Zhang, B.; Richards, K.; Elbrecht, A.; Johnson, B. A.; Zhou, G.; Doebber, T. W.; Biswas, C.; Parikh, M.; Sharma, N.; Tanen, M. R.; Thompson, G. M.; Ventre, J.; Adams, A. D.; Mosley, R.; Surwit, R. S.; Moller, D. E. Distinct Properties and Advantages of a Novel Peroxisome Proliferator-Activated Protein γ Selective Modulator. *Mol. Endocrinol*. **2003**, *17*, 662−676.
(44) Berger, J. P.; Leibowitz, M. D.; Doebber, T. W.; Elbrecht, A.; Zhang, B.; Zhou, G.; Biswas, C.; Cullinan, C. A.; Hayes, N. S.; Li, Y.; Tanen, M.; Ventre, J.; Wu, M.; Berger, G. D.; Mosley, R.; Marquis, R.; Santini, C.; Sahoo, S. P.; Tolman, R. L.; Smith, R. G.; Moller, D. E. Novel Peroxisome Proliferator-activated Receptor (PPAR) γ and PPAR δ Ligands Produce Distinct Biological Effects. *J. Biol. Chem.* **1999**, *274*, 6718.
(45) Otwinowski, Z.; Minor, W. Processing of X-ray diffraction data collected in oscillation mode. *Methods Enzymol.* **1997**, *276*, 307−326.
(46) Sack, J. CHAIN—a crystallographic modeling program. *J. Mol. Graphics* **1988**, *6*, 224−235.
(47) McRee, D. E. XtalView/Xfit—A versatile program for manipulating atomic coordinates and electron density. *J. Struct. Biol*. **1999**, *125*, 156−165.
(48) Brünger, A. T,; Kuriyan, J.; Karplus, M. Crystallographic *R*-factor refinement by molecular dynamics. *Science* **1987**, *235*, 458−460.
(49) Brünger, A. T.; et al. Crystallography and NMR system (CNS): A new software system for macromolecular structure determination. *Acta Crystallogr*. **1998** *D54*, 905−921.

JM0502135